Chapter-1

Introduction and Literature Survey

1.1 Introduction

Organic effluents from various chemical industries like pharmaceuticals, dyes, pesticides, resins, adhesives, detergents, tanning agents, fertilizers, lubricants, greases, plasticizers, etc., contribute extensively to natural water pollution[1,2]. Due to their significant impact on human health and environmental ecosystems, effluents containing organic pollutants must be effectively treated before discharge into the environment [3]. Traditional wastewater treatment facilities are typically not equipped to efficiently eliminate these harmful compounds, allowing them to persist in the treated water released into natural water bodies [4]. Various organic wastewater treatment technologies, such as adsorption, membrane filtration, ion exchange, photocatalysis, the Fenton process, and biodegradation, have been developed to eliminate organic pollutants from water [5]. These techniques are classified into separation and chemical degradation techniques. Separation techniques include methods such as coagulation, membrane filtration, ion exchange processes, and adsorption [6,7]. These techniques separate the organic pollutants from wastewater. For example, coagulation produces sludge containing pollutants, and membrane processes generate concentrated pollutant solutions[8,9]. Adsorption is recognized as a practical and cost-effective method for separating pollutants, but issues with separating and recycling adsorbent particles remain significant [10–12]. Superparamagnetic nanoparticles offer a promising solution, as they can be easily separated using a magnetic field and re-dispersed through sonication, enabling

efficient reuse [13,14]. This innovation addresses key limitations, making adsorption more sustainable and efficient for industrial and environmental applications.

Since, adsorption is only a separation technique, the problem of the disposal of organic pollutants remains. Chemical oxidation processes are required for the disposal of organic pollutants by degrading them to non-toxic small aliphatic organic fragments or complete mineralization to CO_2 and H_2O [15,16]. Advanced oxidation processes (AOP) are chemical degradation processes that activate a compound (such as H_2O_2, persulfate ($S_2O_8^{2-}$)) to generate strong oxidants like hydroxyl radicals for enhanced degradation/mineralization of organic molecules [17,18]. Besides these, photocatalysis, and biodegradation are also green chemical oxidation processes [19,20]. Commonly employed AOPs for antibiotic removal include ozonation, ultraviolet (UV) radiation, ultrasound treatment, electron beam irradiation, and various Fenton-based approaches, such as sono-Fenton, photo-Fenton, electro-Fenton, and photo-electro-Fenton methods [21,22]. All these AOPs are sustainable processes, utilizing H_2O_2 as a precursor for generating •OH radicals[22,23]. The photo-Fenton process is one of the most environmentally friendly techniques, as it only requires sunlight and H_2O_2 to drive the reaction [23,24]. Thus, remediation of wastewater should have both separation and organic pollutant degradation parts.

The present thesis investigates the removal of three classes of organic pollutants from aqueous medium. These organic pollutant classes are i) phenol-based compounds, ii) pharmaceuticals, and iii) dyes. Among these, phenol-based compounds are one of the most common organic contaminants in industrial wastewater, originating from pesticide production, paper manufacturing, plastic industries, and oil refineries [25]. For instance, bisphenol A (BPA), extensively used in producing polycarbonate plastics and epoxy resins,

is a major industrial pollutant with an annual production reaching millions of tons[26,27]. The World Health Organization (WHO) has established 0.001 mg/L as the maximum permissible concentration of phenol in drinking water [28,29]. Furthermore, phenolic compounds exhibit toxic effects in humans at concentrations ranging between 10 and 24 mg/L [30].

Likewise, the global use of antibiotics, particularly ciprofloxacin and tetracycline, has risen sharply in recent years, garnering widespread attention [31]. Extensive usage of antibiotics produces significant residues in aquatic environments [32]. The continuous presence of antibiotic traces in natural water bodies, even in minimal amounts, can contribute to the emergence of antibiotic-resistant microorganisms [33]. A recent publication by the World Health Organization (WHO/Europe) emphasized the prevalent non-prescription use of antibiotics throughout the WHO European Region and Central Asia [34].

On the other hand, azo dyes containing chromophore group -N=N- bonded to aromatic rings, represent 60–70% of total dyes consumed in the textile industries in the world [35]. Among synthetic azo dyes, methyl orange (MG) is widely utilized in the textile, leather, and paper industries owing to its bright color and chemical resilience. However, it has emerged as a major environmental concern because of its genotoxic and carcinogenic properties [36]. MG imparts a vivid orange color when released into water bodies, reducing water clarity and disrupting photosynthesis in aquatic plants[36]. Numerous industries release dye-laden effluents containing MG into water bodies with minimal or no prior treatment. This practice results in the accumulation of MG and other dye residues, causing various environmental and health problems.

There is a growing possibility of detecting antibiotics and dyes in our nearby water sources due to improper disposal of hospital waste, routine antibiotic use in humans and

livestock, domestic washing of synthetic fabrics, and discharge from printing/textile workshops. These pollutants often enter drains that lead directly to rivers or lakes without adequate treatment. Notably, the coexistence of antibiotics and dyes in such water samples raises concerns about their potential synergistic or compounded effects on aquatic ecosystems and microbial communities. However, most research has focused on removing single organic pollutants, leaving the study of simultaneous adsorption/co-adsorption or competitive adsorption of multiple organic compounds relatively unexplored[37–41]. This gap has resulted in a scarcity of co-adsorption data. Simultaneously removing more than one pollutant poses additional challenges due to potential interactions between the organic compounds [42].

Based on the preceding discussion of various wastewater treatment techniques, it is evident that pollutant removal through adsorption and co-adsorption, along with degradation via Fenton and photo-Fenton processes, represents a techno-economically viable approach for remediation of water containing organic pollutants. Accordingly, this thesis initially examines the adsorption and co-adsorption behavior of superparamagnetic $NiFe_2O_4$-based nano adsorbents toward organic pollutants. Particular attention is given to understanding the molecular interactions between adsorbates and adsorbents in the presence of abundant solvent molecules. Generally, experimental studies have overlooked the molecular interactions occurring during adsorption. To address this gap, this thesis conducts a combined experimental and computational approach to the simultaneous adsorption of organic pollutants by nano-adsorbents. Computational investigations on such problems include in-depth investigation of adsorbent-adsorbate interactions using large-scale molecular dynamics (MD) simulations and density functional theory (DFT) calculations. Later sections explore the Fenton and photo-Fenton catalytic properties of $NiFe_2O_4$-based nanomaterials through a combination of experimental and computational

analyses. The upcoming sections introduce key adsorption concepts. Subsequent sections introduce crucial heterogeneous Fenton and photo-Fenton catalysis features.

1.2 Adsorption process

Heinrich Kayser, a German physicist, was the first to introduce the term 'adsorption' [43]. Adsorption is a process where substances in liquid, gas, or solid form accumulate on the surface of another material. The substance that accumulates is called the adsorbate, while the surface it attaches to is known as the adsorbent, shown in Fig. (1.1) [44,45]. The adsorption efficiency is greatly affected by several factors that govern the adsorption process, including pressure, temperature, the unique adsorption characteristics of the adsorbent, and the adsorbent's surface area [45]. Typically, an adsorbent is mixed with a solution containing the adsorbate (such as a pollutant), and under certain conditions, the adsorbate binds to the surface of the adsorbent through chemical or physicochemical interactions until equilibrium is established.

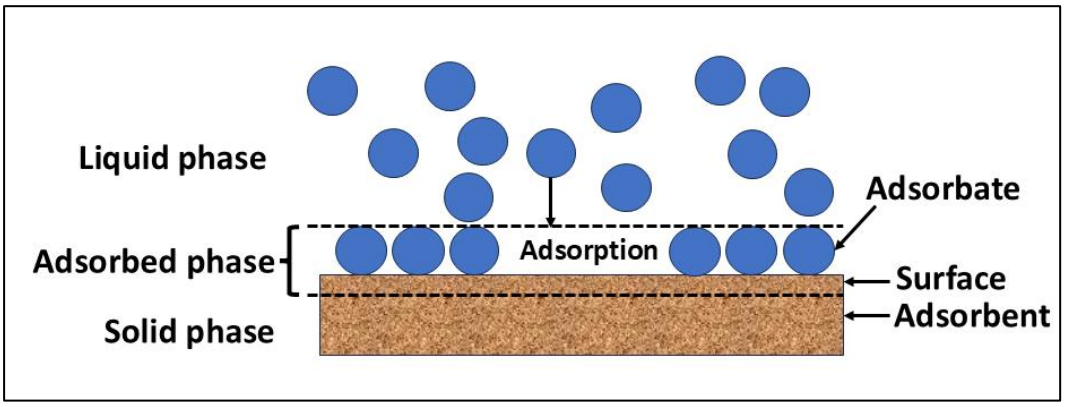

Figure 1.1 The basic terms of adsorption phenomenon.

Adsorption is typically classified into two types based on the nature of the interactions between the adsorbent and the adsorbate: chemisorption and physisorption[45]. Chemisorption is usually an irreversible process, occurring due to the formation of strong chemical bonds between the adsorbate and the adsorbent's surface [44]. In contrast,

physisorption is a reversible process that occurs through weaker intermolecular forces, such as π–π interactions, dipole-dipole interactions, van der Waals forces, and hydrogen bonding between the adsorbate and the adsorbent [45]. The adsorption phenomenon gives rise to the following interactions.

1) Adsorbate-adsorbent interaction, 2) Adsorbate-adsorbate interaction,

3) Adsorbate-solvent interaction, 4) Adsorbent-solvent interaction,

For efficient adsorption, the interaction between the adsorbate and the adsorbent must be stronger than the interactions between adsorbate molecules or between the adsorbate and the solvent[46]. However, entropic factors, influenced by the size and morphology of the adsorbate molecules, also play a significant role. Since this thesis focuses on organic pollutant removal from water, all subsequent discussions will consider water as the solvent.

The adsorption performance of any adsorbent is quantitatively calculated using the parameters known as 'equilibrium adsorption capacity' and 'percentage removal efficiency'. The equilibrium adsorption capacity signifies the maximum amount of solute that can be removed from the mixture per gram of the adsorbent[44]. Equation (1.1) represents the equilibrium adsorption capacity (q_e, mg/g).

$$q_e = \frac{(C_0 - C_e)V}{m} \quad (1.1)$$

In Eq. (1.1), C_0 and C_e are the initial and equilibrium concentration (mg L^{-1}) of the solute, respectively, m (in grams) is the amount of adsorbent added in the solution, and V (in liters) is the volume of adsorbate solution.

Eq. (1.2) denotes the time-dependent adsorption capacity (q_t, mg/g).

$$q_t = \frac{(C_0 - C_t)V}{m} \quad (1.2)$$

In Eq. (1.2), C_t is the concentration (mg L^{-1}) of the solute at time *t*. The rest of the symbols in this equation have the same meaning as in equation (1.1).

Eq. (1.3) represents the percentage removal efficiency (% RE),

$$\% RE = \frac{(C_0 - C_e) * 100}{C_0} \quad (1.3)$$

The all the symbols present in equation (1.3) have the same meaning as in equation (1.1).

1.2.1 Adsorption kinetics models

Adsorption kinetics are crucial for understanding the adsorption rate and the mechanisms involved, which include mass transfer, diffusion, and surface reactions on the adsorbent. Typically, adsorption occurs in three stages: (1) the movement of adsorbate molecules to the external surface of the adsorbent, (2) their diffusion through the boundary layer, and (3) the final diffusion from the adsorbent surface into internal adsorption sites through pore diffusion [47]. Kinetic profiles generally show a rapid initial increase in adsorption capacity, which gradually slows down before reaching equilibrium over time [47]. The rapid uptake is attributed to the abundance of available active sites at the beginning. As adsorption progresses, these sites become increasingly occupied, leading to a slower rate of adsorption in the later stages. For achieving more information about the rate controlling stages, mainly two kinetics models, including Lagergren's pseudo-first-order, and Ho's pseudo-second-order models, were applied [48,49].

1.2.1 (a) Pseudo-first-order (PFO) kinetic model

The PFO kinetic model is also referred to as the Lagergren rate equation, assumes that the adsorption rate is governed by the diffusion of the adsorbate across the surface of the adsorbent [50]. Equation 1.4 denotes the nonlinear equation for PFO kinetic model.

$$q_t = q_e(1 - e^{-k_1 t}) \quad (1.4)$$

In eq. 1.4, q_e and q_t *in* mg g^{-1} units represent the adsorption capacity at equilibrium and at time **t**, respectively. The rate constant of PFO kinetic model is represented by k_1 (min^{-1}).

1.2.1 (b) Pseudo-second-order (PSO) kinetic model

The PSO adsorption kinetics model is applied to describe adsorption processes that take a longer time to occupy the adsorption sites or reach equilibrium. It assumes that the adsorption rate is governed by the interactions between the adsorbate and the active sites on the adsorbent surface throughout the entire process[50]. Equation 1.5 represents the nonlinear equation for the PSO kinetic model.

$$q_t = \frac{k_2 q_e^2 t}{(1+k_2 q_e t)} \quad (1.5)$$

In eq. 1.5, the PSO rate constant of the PSO kinetic model is denoted by k_2 ($g.mg^{-1}.min^{-1}$). The other symbols in this equation carry the same meaning as those in equation 1.4. The suitability of the adsorption mechanism for each model is evaluated using the coefficient of determination (R^2).

Nevertheless, extending this inference for simultaneous adsorption from a binary adsorbate solution may not be correct. Note that, to our knowledge, there are no binary adsorption kinetics models in literature. Hence, no attempt has been made to fit the binary kinetics adsorption data to any kinetics equation.

1.2.2 A brief review of adsorption isotherm models

Adsorption isotherms are crucial for understanding the interaction between solutes and adsorbents, as well as for optimizing the effective use of adsorbents [51]. The adsorption isotherm represents a plot that illustrates the distribution of solute concentration between the mobile liquid/ gas phase and the stationary solid phase at a constant temperature [47]. In

short, the adsorption isotherms illustrate the relationship between the equilibrium adsorption capacity and the equilibrium concentration of the adsorbate (Ce). To determine this relationship, the experimental equilibrium data are analyzed using various mathematical models known as adsorption isotherm models. Till date, there are various adsorption isotherms models available in the literature [45]. Among them, Langmuir, Freundlich, and Langmuir-Freundlich isotherm models are mostly utilized to predict the adsorption phenomenon. These models are discussed in the subsequent section.

1.2.2 (a) Langmuir isotherm model

Langmuir adsorption is one of the most basic models in studying the effect of adsorption on phase behavior, introduced by Langmuir (1918) [52]. Langmuir isotherm is commonly used to represent monolayer adsorption on homogeneous surfaces [53]. The primary assumptions of the Langmuir isotherm model include: (1) adsorption takes place at specific binding sites located on the surface of the adsorbent [54], (2) All adsorption sites present on the surface of the adsorbent are identical [54] (3) The adsorbent surface is covered with a monolayer of adsorbed molecules [55], and (4) The adsorbed molecules on the adsorbent surface do not interact with each other [55]. Equation 1.6 represents the nonlinear equation of Langmuir adsorption isotherm;

$$q_{e}= \frac{q_m \times k_l \times C_e}{1+k_l \times C_e} \qquad (1.6)$$

In equation 1.6, q_e and C_e denote the amount of adsorbate adsorbed on the adsorbent (mg/g) and the concentration of adsorbate present in the solution at equilibrium condition (mg/L), q_m represents the maximum monolayer adsorption capacity (mg g^{-1}), k_l indicates the Langmuir constant related to the affinity of binding sites (L mg^{-1}).

1.2.2 (b) Freundlich isotherm model

Unlike the Langmuir isotherm, this empirical model can be used to multilayer adsorption on heterogeneous surfaces [56]. The Freundlich equation (Eq. (1.3)) is a fully empirical equation used to describe equilibrium data [57]. It assumes the adsorbent surface is heterogeneous, with varying adsorption sites that possess different adsorption energies [56]. Equation 1.7 represents the nonlinear equation of Freundlich adsorption isotherm;

$$q_{e=}k_f C_e^{1/n} \qquad (1.7)$$

In equation 1.7, $\mathbf{k_f}$ is the maximum adsorption capacity of targets in Freundlich isotherm (L mg^{-1}) and '***n***' is a constant representing adsorption intensity (where n>1). When $0 < 1/n < 1$, adsorption is considered favorable. and unfavourable adsorption occurs when $1/n > 1$ and is irreversible at $1/n = 1$ [57,58]. The Freundlich model fits well only in low or intermediate concentration ranges**.**

1.2.2 (c) Langmuir-Freundlich isotherm model

The Sips isotherm, also known as the combined Langmuir-Freundlich isotherm (a three-parameter model), is ideal for predicting adsorption on heterogeneous surfaces, effectively overcoming the limitations of the Freundlich model, particularly regarding the increased adsorbate concentration [59,60]. This model reduces to the Freundlich model at low adsorbate concentrations and predicts Langmuir or monolayer adsorption at higher concentrations [61]. The adsorption sites are heterogeneous, but this model doesn't consider any adsorbate-adsorbate interaction. The Langmuir–Freundlich isotherm was initially proposed for gas adsorption on heterogeneous solids (Eq. 1.8), but its analog has been widely used for adsorption from the liquid phase.

$$q_{e=}\frac{q_m k C_e^{1/n}}{1+kC_e^{1/n}} \qquad (1.8)$$

In equation 1.8, ***k*** indicates the Langmuir-Freundlich constant related to the affinity of binding sites (L mg^{-1}).

1.3. Adsorption isotherms models for co-adsorption cases

Standard Langmuir, Freundlich, and Langmuir-Freundlich isotherm models are unsuitable for multi-adsorbate systems. Therefore, the multi-component extended versions of these models are employed to fit the co-adsorption isotherm data. Equations 1.5a to 1.7b represent expressions for the Extended Langmuir (EL) isotherm, Extended Freundlich (EF) isotherm, and Extended Langmuir-Freundlich (ELF) isotherm, respectively [62–64].

1.3.1. Extended Langmuir isotherm model

The Extended Langmuir (EL) isotherm for multicomponent adsorption is a generalization of the Langmuir isotherm to describe the adsorption of multiple adsorbates on a solid surface [62,65]. The key assumptions of this model are; (1) All the active sites on the adsorbent are of one type only [62], (2) The model assumes that there is no interaction between the different adsorbate molecules [65], (3) The adsorption energy is the same for all sites for a given adsorbate [65]. Equation 1.5 give isotherm relation for this multi-component adsorption model in system having j=1, 2,,…,i,…N, where N is the total number of the adsorbate present in the multi adsorbate system.

$$q_{ei} = \frac{(q_{mi} b_i Ce_i)}{(1+\sum_{j=1}^{N} b_j Ce_j)} \qquad (1.5)$$

In Eq. (1.5), q_{mi} represents the maximum monolayer adsorption capacity(mg.g^{-1}) for adsorbate ‘i’; b_i indicates Langmuir constants (L.mg^{-1}) for adsorbate ‘i’ in multi-adsorbate system.

1.3.2. Extended Freundlich adsorption isotherm

The extended empirical Freundlich isotherm combines single-component isotherm constants with correlative constants derived from multicomponent equilibrium data [63]. The model is used for heterogeneous systems [66]. It includes interaction between different adsorbed molecules [66]. The equation (1.6) represents the nonlinear extended Freundlich adsorption isotherm for a multicomponent system as follows;

$$q_{ei} = \frac{k_i Ce_i^{((1/n_i)+x_i)}}{(Ce_i^{x_i} + \sum_{j \neq i} y_i \, Ce_j^{z_i})} \qquad (1.6)$$

In Eq. (1.6), k_i represents the Freundlich constant related to the affinity of the binding sites ($L.mg^{-1}$); n_i indicates constant representing adsorption intensity (where $n_i > 1$); x_i, y_i, z_i denotes binary correction coefficients.

1.3.3. Extended Langmuir-Freundlich (ELF) adsorption isotherm

The ELF adsorption isotherm for a binary adsorbate system describes competitive adsorption of two or more components onto heterogeneous surfaces, where surface heterogeneity and competition play significant roles [64]. It combines features of the Langmuir and Freundlich isotherms, accommodating surface heterogeneity and saturation effects. The model assumes that both adsorbates compete for the same adsorption sites, and adsorption occurs as a monolayer without interactions between adsorbed molecules[64]. The equation (1.7) for ELF adsorption isotherm can be represented as;

$$q_{ei} = \frac{(q_{mi} b_i C_{ei}^{1/n_i})}{(1 + \sum_{j=1}^{N} b_j C_{ej}^{1/n_j})} \qquad (1.7)$$

In Eq. (1.7), n_i and n_j indicate constant representing adsorption intensity (where n_i, $n_j > 1$); b_i and b_j represent LF affinity constants ($L.mg^{-1}$) for adsorbate 'i' and 'j', respectively.

Adsorption plays a crucial role in pollutant separation and is a prerequisite for the effectiveness of heterogeneous catalysts. The performance of all heterogeneous catalysis

methods is influenced by the nature and extent of reactant adsorption on the catalyst. Therefore, the following section explores heterogeneous catalytic reaction mechanisms, including this perspective.

1.4 Heterogeneous Fenton catalysis

The classical Fenton reaction [Fenton, 1894] is a homogeneous process that rapidly generates hydroxyl radicals (•OH) through the reaction of ferrous ions (Fe^{2+}) with hydrogen peroxide (H_2O_2) under acidic conditions as represented in Equation (1.8)[67,68]. Acidic pH is essential because, at higher (basic) pH levels, ferrous ions tend to react with hydroxyl ions to form ferric hydroxide [$Fe(OH)_3$], which is insoluble and precipitates out as sludge [68]. This not only reduces the availability of iron for the Fenton reaction but also complicates the process due to sludge formation. Therefore, maintaining an acidic environment enhances the efficiency of hydroxyl radical production and minimizes sludge generation. The reaction begins with the fast reduction of H_2O_2 by Fe^{2+} ions, which are simultaneously oxidized to Fe^{3+} ions. The next step in the process involves regenerating the catalyst, Fe^{2+} ions, but this step is significantly slower than the initial one (Equation 1.9). The rate constant for hydroxyl radical generation (Eq. 1.8) is much higher than for catalyst regeneration (Eq. 1.9), accumulating Fe^{3+} salts as sludge. Furthermore, a continuous supply of Fe^{2+} salts is required to sustain the reaction.

$$Fe^{2+} + H_2O_2 \rightarrow Fe^{3+} + {}^{\bullet}OH + OH^-,\ k_1 = 40\text{-}80\ m^{-1}s^{-1} \quad (1.8)$$

$$Fe^{3+} + H_2O_2 \rightarrow Fe^{2+} + HO_2^{\bullet} + H^+,\ k_2 = 0.001\text{-}0.01\ m^{-1}s^{-1} \quad (1.9)$$

Heterogeneous Fenton and Fenton-like reactions are terms used to describe Fenton processes involving heterogeneous catalysts [69]. In this variation, the traditional dissolved iron salt used in the classical Fenton method is substituted with solid iron-based catalyst particles or nanoparticles [69]. A heterogeneous Fenton system can produce hydroxyl radicals

(•OH) through two distinct pathways. It may involve a proper heterogeneous catalytic mechanism or a homogeneous Fenton reaction resulting from the leaching of iron ions from the solid catalyst [69]. Lin and Gurol (1998) introduced a widely recognized mechanism 1998 for the heterogeneous catalytic breakdown of H_2O_2 by examining its interactions with a solid iron oxide catalyst, specifically goethite [70]. In this mechanism, $\equiv Fe^{III}$ denotes surface-bound iron. Initially, H_2O_2 interacts with the goethite surface ($\equiv Fe^{III}$ OH) to form a surface-bound complex $(H_2O_2)_s$ (Eq. 1.10). A ligand-to-metal charge transfer subsequently produces a transition state complex ($\equiv Fe^{II}$ $\bullet O_2H$) (Eq. 1.11). This complex then dissociates, generating hydroperoxyl radicals (Eq. 1.12), followed by the formation of hydroxyl radicals (•OH) in the presence of ≡FeII and H_2O_2 (Eq. 1.13). The mechanism also illustrates the cyclic transformation between Fe(III) and Fe(II) on the surface, validating goethite's role as a heterogeneous catalyst.

$$\equiv Fe^{III}\text{-}OH + H_2O_2 \leftrightarrow (H_2O_2)_s \quad (1.10)$$

$$(H_2O_2)_s \leftrightarrow (\equiv Fe^{II} \bullet O_2H) + H_2O \quad (1.11)$$

$$(\equiv Fe^{II} \bullet O_2H) \rightarrow \equiv Fe^{II} + HO_2 \bullet \quad (1.12)$$

$$\equiv Fe^{II} + H_2O_2 \rightarrow \equiv Fe^{III}\text{-}OH + \bullet OH \quad (1.13)$$

Here, ≡Fe indicates surface iron and $(H_2O_2)_s$ denotes the complex formed by the interaction of H_2O_2 and goethite surface.

In addition to the pure heterogeneous Fenton process, the reaction rate is further enhanced by the homogeneous Fenton pathway due to iron leaching from the solid catalyst. Some researchers have reported iron leaching from the Amberlyst-15 ion-exchange resin during kinetic modelling of 4,6-dinitro-o-cresol (DNOC) degradation[71–74]. The degradation

rate increased with hydrochloric acid addition due to higher ferrous ion leaching at lower pH. Furthermore, pH variations influenced metal ion leaching over time, and even trace concentrations (μM/ppm) of dissolved metal ions enhanced the degradation rate in the heterogeneous Fenton system [69].

In the Fenton process, the pH strongly affects the interaction between Fe^{2+} and H_2O_2. The optimal pH is around 3. At pH below 1, the reaction mainly involves the oxidation of Fe^{2+} by H_2O_2. Degradation efficiency decreases at pH below 3 due to the formation of $[Fe(H_2O)_6]^{2+}$ complexes, which slow the reaction, and the solvation of H_2O_2, which reduces its reactivity [75]. At pH above 3, excess H_2O_2 can decompose. Similarly, at still higher pH levels, inactive iron oxyhydroxides form, ferric hydroxide precipitates, and H_2O_2 decomposes faster, reducing the reactivity of the Fenton reagent [75]. This decreases the availability of free iron ions, leading to fewer •OH radicals and a lower oxidation potential. As a result, Fenton reactions are less effective at low and high pH.

1.4 Heterogeneous photo-Fenton catalysis

A photo-Fenton reaction is one in which light of a suitable wavelength can generate hydroxyl radicals from H_2O_2 [75]. Thus, UV light irradiation can cleave H_2O_2 and produce hydroxyl radicals that can be used to oxidize organic molecules. Another way to generate hydroxyl radicals from H_2O_2 using light is by a visible light photocatalyst that can reduce H_2O_2 [19]. Such a material is classified as a heterogeneous photo-Fenton catalyst or photocatalyst. Since it is a photocatalytic process, light must have an energy greater than the band gap of the photocatalyst[76]. Irradiation by light of suitable wavelength photo excites electrons from the valence band (VB) to the photocatalyst's conduction band (CB). The heterogeneous photo-Fenton process using visible light has gained significant attention, as nearly 45% of solar radiation is in the visible range, making photocatalytic processes that

utilize visible light crucial [77]. The latter is possible if the band gap is less ~2.8 eV (in the visible range of the solar spectrum). Semiconductor materials with medium bandgaps are preferred as they combine use of visible light for photoexcitation with appropriate VB and CB positions. The CB position of photocatalyst should be more negative (per electrochemical series) than the reactant targeted for reduction. Similarly, the VB position should be more positive than the reduction potential of the reactant to be oxidized [78]. Hence, photoexcited CB electrons reduce H_2O_2 to hydroxyl radicals and hydroxide anions. Loss of electrons at the CB oxidizes Fe in the photocatalyst from its +2 to the +3 oxidation state, while it is regenerated by quenching the photo-excited holes in the VB of the photocatalyst [79]. Figure 1.2 shows the general mechanism of heterogeneous photo-Fenton catalysis process. This light-driven regeneration reduces the need for frequent catalyst regeneration or replacement, enhancing the efficiency and longevity of the photocatalytic process. This thesis explores the Fenton and photo-Fenton activity of pure $NiFe_2O_4$ and $NiFe_2O_2$-based nanomaterials.

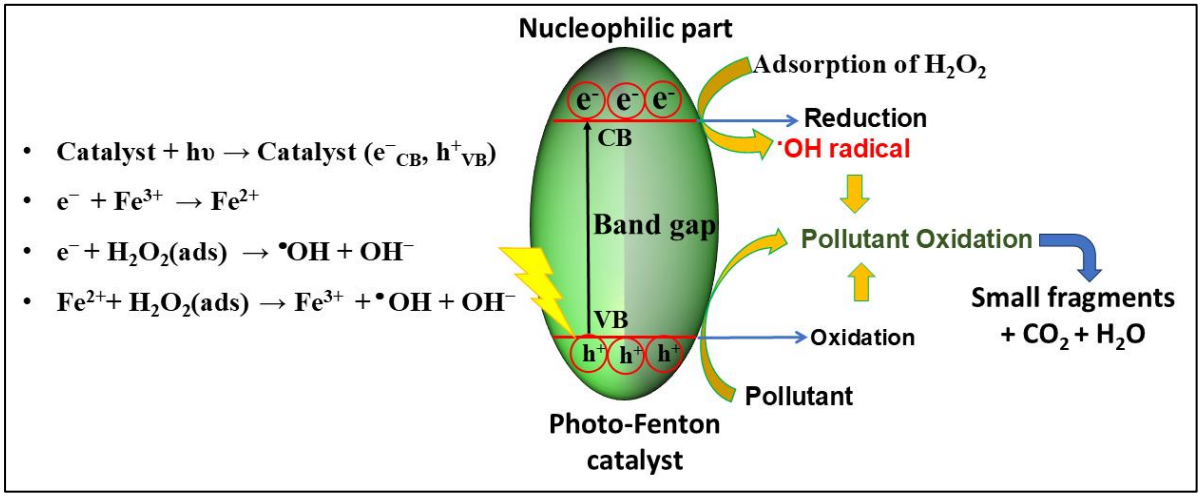

Figure 1.2 The general mechanism of heterogeneous photo-Fenton catalysis process.

1.5 Research gap based on literature survey

Nonmagnetic adsorbents and catalysts pose challenges in wastewater treatment due to their separation and recovery difficulties after use. Their removal is inefficient and often requires additional filtration or chemical treatment[80]. This can lead to incomplete removal, leaving residues of adsorbent in treated water and contributing to secondary pollution[81]. Moreover, residual catalysts or adsorbents may react with other compounds, forming toxic by-products. In contrast, superparamagnetic materials offer easier separation using external magnets, minimizing secondary contamination and enabling reusability. It is critical to highlight the requirement of superparamagnetic particles instead of magnetic materials for this purpose. Superparamagnetic particles can be magnetized in the presence of a magnetic field and demagnetized by removing the field. In contrast, if the particles are ferromagnetic, magnetization is irreversible and requires considerable energy to reverse and regenerate the non-aggregated adsorbent or catalytic nanoparticles. Therefore, developing superparamagnetic adsorbents and catalysts is crucial for sustainable and environmentally friendly wastewater treatment processes.

Metal ferrites have attracted considerable interest owing to their outstanding magnetic, catalytic, and photocatalytic characteristics. They also exhibit remarkable chemical stability, making them suitable for various practical applications [82]. Most ferrite materials exhibit medium-range bandgaps (~ 2 eV), utilizing a substantial range of solar radiation, and thus can exhibit efficient photocatalytic activity [82,83]. Metal ferrites exhibit notable limitations. For instance, $CoFe_2O_4$ has potential toxicity issues due to cobalt, along with lower photocatalytic efficiency[84]. $ZnFe_2O_4$, and $MnFe_2O_4$ while capable of visible light absorption, suffers from weak magnetic properties and poor structural stability, limiting its reusability[83]. Magnetite (Fe_3O_4), although highly magnetic and widely used, has a very narrow band gap (~0.1 eV), which makes it susceptible to fast charge recombination and limits its photocatalytic performance under visible light [85]. These limitations

collectively highlight the advantages of $NiFe_2O_4$ as a more efficient and reliable material for environmental remediation applications[81,86,87].

Among the many ferrite materials, $NiFe_2O_4$ can be considered a superior ferrite for dual functions as an adsorbent and photocatalyst due to its favorable physicochemical properties, including a high surface area, strong magnetic response for easy separation, excellent chemical stability, and a relatively narrow band gap (~1.6-2.2 eV) that enables its photoexcitation by efficient utilization of visible light [88–90]. Structurally, $NiFe_2O_4$ possesses an inverse spinel structure with the general formula $(Fe^{3+})[Ni^{2+}Fe^{3+}]O_4$, where Fe^{3+} ions are distributed between both tetrahedral and octahedral sites, while Ni^{2+} preferentially occupies the octahedral sites[81]. This specific cation distribution influences its electronic structure, magnetic behavior, and catalytic performance. Given these advantages, this thesis focuses on the adsorption and photocatalytic properties of $NiFe_2O_4$ nanomaterials. However, because of their fine sizes, the high surface energy $NiFe_2O_4$ particles often lead to particle aggregation, resulting in larger aggregates with reduced surface area, lower surface energy, and diminished adsorption [81]. Conversely, the adsorption properties of pristine $NiFe_2O_4$ are often limited due to its low surface area and lack of active sites, which further hinder its overall effectiveness [91]. These characteristics hinder its efficiency in adsorption-based applications. Liang et.al. found that only ~49.3% removal of tetracycline antibiotic by pure $NiFe_2O_4$, which was nearly half of the adsorption performance of the $NiFe_2O_4$/biochar (NFO/BC) composite under same condition [92]. This occur because the surface area of pure $NiFe_2O_4$ was 1/3rd of that of NFO/BC composite. Lingamdinne et.al. demonstrated that the adsorption of radioactive elements, Uranium (VI) and Thorium (IV) by pure $NiFe_2O_4$ was approximately 45.5 and 34.6 mg g^{-1}, whereas on functionalizing the pure $NiFe_2O_4$ with reduced graphene oxide, the adsorption capacity was increased by ~2.5 times [93]. This low adsorption capacity of pure $NiFe_2O_4$ was observed due to lack of its low

surface area and smaller number of active sites. Similarly, in several previous reports, the low adsorption performance of bare $NiFe_2O_4$ was observed [94]. On the other hand, Fu et. al. reported that pure $NiFe_2O_4$ showed poor photocatalytic degradation (9.1%) of rhodamine [95]. Their photocatalytic results demonstrate that the incorporation of 2D-MoS_2 with $NiFe_2O_4$ greatly improves the adsorption of visible-light and facilitates the transferring and charge separation of photogenerated electrons and holes. Xiong et. al. found that bare $NiFe_2O_4$ had negligible ~8% photocatalytic degradation efficiency for phenol molecules [96]. Many studies reported the poor photocatalytic activity due to rapid recombination of charge carriers [97,98].

As per the literature survey, there is one way to modify the particle surface by surface functionalization or stabilization. Surface modification of $NiFe_2O_4$ with organic molecules can effectively prevent particle aggregation, enhance its stability, and improve its adsorption performance. This surface modification introduces more functional groups, facilitating improved adsorption of pollutants. The adsorbent and photocatalytic properties of $NiFe_2O_4$ can also be improved by forming composites with other phases. Several researchers have employed various supporting materials, including organic moieties, surfactants, polymers, biomolecules, inorganic compounds, and carbon-based materials, to modify the surface properties of $NiFe_2O_4$ nanoparticles [94–98].

Previous studies on $NiFe_2O_4$-based materials have extensively explored their adsorption capabilities for the removal of individual organic pollutants, including phenolic compounds, antibiotics, and dyes. For example, Zhu et.al. synthesized a $NiFe_2O_4$/ZnO composite and reported a high adsorption capacity of 221.73 mg g^{-1} for Congo red, due to an increased surface area and the presence of diverse adsorption sites[99]. Similarly, Bayat et al. enhanced the adsorption performance of $NiFe_2O_4$ by surface modification using zeolite

and sodium alginate, achieving effective removal of methylene blue[100]. In another study, Livani et.al. developed a $NiFe_2O_4$/activated carbon composite and demonstrated excellent adsorption efficiency, successfully removing Direct Red 38 and Direct Blue 78 within just 20 minutes [101]. These findings emphasize the versatility and high efficiency of $NiFe_2O_4$-based composites in the adsorption of a wide range of organic pollutants.

Another way of mitigating the above-stated disadvantages of $NiFe_2O_4$ as adsorbents or photocatalysts is by modifying its crystal structure through doping. For instance, incorporating or doping foreign elements into the crystal structure of nickel ferrite can alter its electronic properties (bandgap and band positions), generate extra binding sites, and adsorption properties for targeted pollutants [102,103]. Moreover, such doping may enhance nickel ferrite's surface area and porosity. The doping of ferrite phases gives rise to particles with adsorption properties different from the parent phase. The size or valence difference between dopant cation and making pure phase induce defects in the pure phase. These defects are due to stress and strains induced by mismatches in sizes and coordination number of the dopant cation. Doping also introduces sites with electron distributions that differ from those otherwise. Such defects are high-energy potential adsorption sites. Thus, doping gives birth to different types of defect sites, in addition to the parent phase adsorption sites. Different energies and specificities of sites in doped nanoparticles make them particularly suitable for co-adsorption or simultaneous adsorption of organic molecules with different functionalities. While the adsorption of most organic molecules on $NiFe_2O_4$ particles is average or poor, the adsorption behavior can be changed by appropriate doping. Nevertheless, there are few published reports in the literature on the adsorption behavior of doped $NiFe_2O_4$ nanoparticles. Chen et.al. reported the excellent adsorption capacity (132 mg g^{-1}) of cobalt doped $NiFe_2O_4$ adsorbent [104]. In another report, Luo et.al. demonstrated that the adsorption capability of Congo red on $Ni_{(1-x)}Mn_xFe_2O_4$ has

a great enhancement due to change in charge distributions by the suitable doping of Mn^{2+} ions [105]. Note that dilute solid-state doping is preferred in such cases because higher doping percentages may not be compatible with the parent phase structure, and phase separation may occur. Moreover, a higher doping percentage could also destroy the desirable superparamagnetic properties of the adsorbent. In this context, the simultaneous adsorption or co-adsorption of pollutant mixtures from aqueous solutions remains unexplored mainly [64,106,107]. Investigating the molecular-level adsorption mechanisms is crucial for addressing challenges associated with co-adsorption and optimizing the removal of complex pollutant mixtures.

Conventional adsorption isotherms offer limited molecular-level insights, particularly for composite or doped adsorbents having diverse adsorption sites. Moreover, adsorption data often exhibit a good fit with multiple traditional isotherm models, complicating the derivation of definitive conclusions about the adsorption mechanism based solely on such analyses. Few experimental studies focus on elucidating adsorption mechanisms by analyzing adsorbate-adsorbent interactions[106,108]. For instance, Liu et al. synthesized functionalized $NiFe_2O_4$, which exhibited remarkable dual functionality. It not only enabled the rapid simultaneous removal of co-existing metal ions (Cu^{2+}, Cd^{2+}, Cr^{3+}, and Zn^{2+}), but also efficiently adsorbed fluoroquinolones (FQs)[109]. However, most of the researchers have utilized the traditional adsorption isotherm models to understand the adsorption mechanism. These mechanisms, including covalent bonding, π–π stacking, electrostatic forces, hydrogen bonding, acid-base interactions, complexation, chelation, hydrophobic effects, and ion exchange, remain poorly understood due to their complexity arising from the simultaneous occurrence of multiple interactions. Spectroscopic techniques such as UV-Vis, FTIR, Raman, and XPS provide structural insights into adsorption mechanisms.

However, they often struggle to capture interfacial complexities and are less effective in explaining molecular-level dynamics.

Computational methods effectively investigate inter/intramolecular interactions in adsorption systems. Techniques such as classical molecular dynamics (MD) simulations and Density Functional Theory (DFT) provide complementary insights into the molecular-level mechanisms underlying the adsorption process [110,111]. MD simulations have been employed to study ferrite-based adsorbents, shedding light on their interactions with organic contaminants[112,113]. However, classical MD simulations have predominantly focused on systems with a single adsorbate. The computational understanding of simultaneous and competitive adsorption involving multiple adsorbates on $NiFe_2O_4$ based adsorbents remains limited, highlighting the need for further exploration[114–116]. Theoretically, a comprehensive investigation is essential to resolve the adsorption mechanism. The following questions highlight key aspects that must be addressed to elucidate the interfacial processes during adsorption and co-adsorption using MD simulation and DFT studies.

1. How do adsorbate molecules adsorb to the adsorbent surface in the presence of many explicit water molecules?
2. How does each organic pollutant's (adsorbate) atom interact with specific atoms on the adsorbent surface?
3. How does the orientation and alignment of reactant molecules relative to the adsorbent surface affect their adsorption behavior?
4. What is the molecular level co-adsorption mechanism?

1.6. Research gap based on literature survey on Fenton and photo Fenton activity

An efficient photocatalytic process relies on key factors such as band gap, band edge positions, recombination rate, and reactant adsorption properties of the photocatalyst. Oxidation and reduction reactions are facilitated by photoinduced electrons and generated holes, producing reduced and oxidized products, respectively. This occurs only when the target species adsorb onto the photocatalyst surface. The reactant to be oxidized should adsorb to the electrophilic portion of the photoexcited photocatalyst. More specifically, for photo-Fenton reactions, it is essential to determine whether the nucleophilic sites of the photocatalyst actively interact with H_2O_2 in its photo-excited state or not.

Given the above objective, this study aims to integrate Density Functional Theory (DFT) calculations with experimental investigations to elucidate the interfacial phenomena involved in the photo-Fenton reaction mechanism on the catalyst surface. Density Functional Theory (DFT) methods give valuable insight into the mechanism of joining of two components in a composite along with its structure optimization. Along with this, it also investigates the optimum dopant position in a doped semiconductor. These quantum chemical calculations also provide information about adsorption and interaction of individual reactants with different sites on the photocatalyst surfaces, bond activation and cleavage during chemical reactions. Parallelly, extensive experimental studies will provide a robust framework for validating computational predictions.

Pristine $NiFe_2O_4$ exhibits relatively weak photocatalytic performance, particularly in the visible light region, due to the rapid recombination of photo-induced electron-hole pairs. This limitation can be addressed by doping $NiFe_2O_4$ with appropriate cation doping, causing change in the band structure of the material. The latter include alteration in the band gap, band positions, and charge separation. Moreover, as detailed in the previous section, it also affects the adsorption properties of the material. For instance, Meena et al.

synthesized Ce-doped $MnFe_2O_4$, where cerium ions (1.02 Å), possessing a larger ionic radius, replaced the smaller Fe ions (0.64 Å) at octahedral sites [117]. This substitution induced the formation of oxygen vacancies within the lattice. Furthermore, Ce^{2+} doping resulted in the formation of a new CB, facilitating the migration of photogenerated electrons to trapping regions of MFO under solar irradiation. This enhanced charge separation significantly suppressed electron–hole recombination. As a result, the Ce-doped MFO (3 mol%) exhibited superior photocatalytic activity, achieving degradation efficiencies 1.5 and 1.67 times higher for methylene blue (MB) and Alizarin Red (AR) dyes, respectively, compared to pristine $MnFe_2O_4$. Similarly, Fang et al. synthesized carbon-doped $ZnFe_2O_4$ with abundant surface oxygen vacancies and lattice defects, induced by the incorporation of carbon atoms into the crystal lattice[118]. These defects introduced in-band states within the band gap, forming defect energy levels that promoted efficient charge separation and multi-channel electron transfer. Consequently, the photocatalyst exhibited enhanced performance, achieving 90.8% degradation of tetracycline hydrochloride.

In another study, Liu et al. developed a $NiFe_2O_4$/g-C_3N_4 heterojunction photocatalyst for the photo-Fenton TC degradation [119]. Compared to the individual components, the 10% $NiFe_2O_4$/g-C_3N_4 composite exhibited significantly improved degradation efficiency, achieving 94.5% removal within 80 minutes. This enhancement was attributed to the improved visible-light absorption and more effective separation of photogenerated charge carriers facilitated by the heterojunction structure. Similarly, Wen et al. constructed a macroporous $NiFe_2O_4$/g-C_3N_4 composite photocatalyst for the photo-Fenton degradation of tetracycline[120]. This composite exhibited a rate constant 5.4 times higher than that of pure $NiFe_2O_4$. The enhanced catalytic performance is primarily attributed to the increased specific surface area and active sites, the effective charge

separation enabled by the heterojunction structure, and the improved Fe^{3+} to Fe^{2+} reduction facilitated by photogenerated electrons, which accelerates the photo-Fenton reaction.

Hence, all three effects of doping significantly enhance the photocatalytic efficiency of the semiconductor for degrading organic contaminants. Similarly, joining the $NiFe_2O_4$ phase to another semiconductor nanomaterial with the condition that the band positions of the two components are staggered relative each other, enhances the possibility of charge separation and lifetime of the excited species. Besides, the incorporation of another component also means that photocatalytic reactions that were hindered by poor adsorption have better likelihood of occurrence.

1.7. The objective of this thesis

The literature survey presented in the preceding section highlights experimental studies employing nickel ferrite-based nanomaterials as adsorbents and catalysts for the removal of various organic pollutants from wastewater. However, the interfacial mechanisms involved in simultaneous adsorption and heterogeneous Fenton catalysis using these materials remain inadequately understood. Moreover, there is a pressing need for an integrated approach that combines experimental and computational studies to unravel these interfacial interactions. Accordingly, this thesis aims to address these critical research gaps through the following objectives.

i) The first problem tackled in the thesis is the adsorption of phenolic pollutants on the $NiFe_2O_4$ (311) surface in the presence of many water molecules by large-scale classical MD simulations. This study does not have any experimental parts. It is entirely an MD study. The results of these investigations are qualitatively compared with the experimental results available in the literature.

ii) The next objective is to investigate the co-adsorption behavior of graphene oxide (GO) and superparamagnetic $NiFe_2O_4$ nanoparticle composites toward ciprofloxacin (CIP) and malachite green (MG) in aqueous solutions. To elucidate the molecular-level interactions involved in the co-adsorption process, classical molecular dynamics (MD) simulations are conducted, including analysis through radial distribution functions (RDFs). To elucidate the underlying adsorption mechanisms, experimental results are complemented by classical MD simulations focusing on co-adsorption or competitive adsorption behaviors of $NiFe_2O_4$/GO nanocomposites.

iii) The next objective is to investigate the co-adsorption or simultaneous removal of two organic pollutants, CIP and MG, by Mo-doped $NiFe_2O_4$ nanoparticles. Moreover, the initial DFT optimization calculations help find the site occupied by the Mo-dopant in $NiFe_2O_4$ crystal structure. DFT calculations are also carried out to investigate adsorbent-adsorbate(s) interactions. Combining experimental and DFT calculation results helps elucidate the molecular-level adsorption mechanism.

iv) The succeeding objective is to investigate the mechanism of Fenton and photo Fenton catalysis of tetracycline (TC) degradation on Mo-doped $NiFe_2O_4$ nanoparticles. These Mo-doped $NiFe_2O_4$ nanoparticles are prepared experimentally following earlier reports. The location of the Mo dopant in the $NiFe_2O_4$ crystal lattice was determined following earlier experimental and DFT calculations reports. Then, Fenton and photo Fenton reactions for TC degradation are carried out on the prepared nano-catalysts under cool white LED visible light irradiation. Simultaneously, DFT calculations investigate the molecular interactions during the Fenton reaction. Experimental and DFT

calculation results were combined to understand the photocatalytic mechanism in this photo-Fenton process.

v) The final objective was to understand the photo-Fenton degradation of TC antibiotic on AgI/$NiFe_2O_4$ nanocomposite. This study was a necessary prelude to investigate the next goal about the Fenton and photo-Fenton activities of AgI/$NiFe_2O_4$ nanocomposites. A series of AgI/$NiFe_2O_4$ composites with varying AgI contents were prepared by a step-wise precipitation method. Parallelly, the photo-Fenton activity of these photocatalysts was evaluated for tetracycline (TC) degradation under cool white LED visible light irradiation. A combination of experimental studies, and DFT calculations were used to understand the Fenton and photo-Fenton mechanisms operating on these nanocomposites.